JOURNAL OF Applied Polymer SCIENCE

Selective Binding of an Imprinted Polymer Resulted from Controlling Cobalt Coordination to Nitric Oxide

Lili Zhao, Changbao Chen, Jie Zhou
College of Chemistry and Material Sciences, Shandong Agricultural University, Taian 271018, China

Correspondence to: J. Zhou (E-mail: zhoujie@sdau.edu.cn)

ABSTRACT: In this article, the binding characteristics of the imprinted polymer P-1[Co^{II}(salen)] (salen: bis(2-hydroxybenzaldehyde)ethylenediimine) to nitric oxide (NO) have been reported. P-1[Co^{II}(salen)] was characterized by Fourier transform infrared analysis, thermogravimetric analysis, and differential scanning calorimetry. Batch-mode adsorption studies were carried out to investigate binding thermodynamics, kinetics, and selective recognition behavior of P-1[Co^{II}(salen)] to NO. The kinetics study indicates that binding of the polymer to NO fits the first-order reaction kinetics with the rate constant k_1 of 0.087 min^{-1}. Langmuir and Freundlich equations were used to explain the equilibrium character of P-1[Co^{II}(salen)] binding to NO. The r^2 and χ^2 values suggest that total amount of NO bound by P-1[Co^{II}(salen)] can be best fitted by the Langmuir equation. The binding capacity (B_{max}) of P-1[Co^{II}(salen)] was calculated to be 76.28 μmol/g, very close to the experimental value, 75 μmol/g. The thermodynamics and selectivity experiments showed that the affinity of P-1[Co^{II}(salen)] to NO was much higher than carbon dioxide (CO_2) and oxygen (O_2), suggesting that P-1[Co^{II}(salen)] is a promising functional material for NO storage and NO sensing. © 2012 Wiley Periodicals, Inc. J. Appl. Polym. Sci. 000: 000–000, 2012

KEYWORDS: metal complex imprinted polymer; nitric oxide; kinetics; thermodynamics

Received 7 April 2011; accepted 23 March 2012; published online
DOI: 10.1002/app.37772

INTRODUCTION

Synthetic polymer receptors have been increasingly developed as mimics of natural molecular recognition hosts.[1,2] Molecular imprinting is now a well-established and effective method to introduce selective recognition sites, which are complementary to specific template molecules in shape, size, and chemical functional groups, into polymeric materials. This method, which was introduced in 1972 by Wulff and Sarhan[3] and then further expanded by Mosbach and coworkers[4] in 1990s, has attracted increasing interest. Molecular imprinting method involves dissolving template molecules, functional monomers, and largely excess amount of crosslinker in a pore-forming solvent (i.e., porogen), thermally or photochemically initiated polymerization, and subsequent reversible removal of the templates from the resulting polymeric matrix, yielding three-dimensional cavities that are complementary in both shape and chemical functionality to those of the corresponding templates. The high degree of crosslinking enables the microcavities to maintain their shape after removal of the templates, allowing the receptors to selectively recognize and rebind the template molecules.[5] Materials made by this method, that is, molecularly imprinted polymers (MIPs), not only have specific recognition to the template molecules like enzyme and antibody but also have other advantages over normal biological receptors like chemical and physical stability, long working life, high adsorption capacity and selectivity for organic and inorganic solutes, simple and rapid preparation methods, and low detection limits because of less matrix interference effects. Consequently, they are widely applied in diverse fields such as preconcentration, liquid chromatography,[6] solid-phase extraction,[7,8] racemic resolution of drugs,[9] sensing technology,[10] and catalysis.[11]

Metal coordination interaction plays both structural and catalytic roles[12] in nature and has been exploited in the development of molecular recognition systems[13,14] because of its advantages such as stronger interaction, higher stability in polar aqueous–alcohol system, and easier preorganization than hydrogen bonds and Van der Waals interactions. The application of metal-ion-mediated recognition is of great potential for the development of MIPs. Ion-imprinting idea basically starts with the formation of a complex of a given metal ion (serving as a template) with appropriate ligands, which is subsequently mixed with functional monomers and crosslinkers and then

immobilized on a crosslinked polymeric matrix. The obtained polymer after extraction of the metal ions, that is, an ionic imprinted polymer (IIP), has the sites that are complementary to the template ion and shows significantly higher affinity for the template ion over other coexisting metal ions. Therefore, IIPs are generally applied in the fields of molecular recognition,[15,16] catalysis,[17] sensing,[18] preconcentration,[19,20] and selective separation.[21] Moreover, IIPs have a large number of metal sites (~90%) isolated from each other by a porous host.[22] The isolated metal sites prevent the formation of undesirable bimolecular metal-based adducts and thus prolong the function lifetime of the polymers.

Interest in the chemistry of nitric oxide (NO), "Molecule of the Year" in 1992, has been growing rapidly in recent years because of its various functions, ranging from its adverse role in the environment[23] to its importance in biology.[24] The multifaceted biological importance of NO can be divided into three categories: protective, regulatory,[25] and deleterious functions.[26] Yet, the application of NO is limited because of its short lifetime and the difficulty in direct use; one way to address this problem is via creating NO storage-release materials that can be easily adopted in a wide variety of applications. To date, a variety of organic compounds that release NO via decomposition routes have been developed; however, few of them have the capability of binding NO[27] reversibly without releasing toxic byproducts.[28] One promising approach for developing such materials is to covalently immobilize metal nitrosyl (M-NO) complexes within porous polymeric hosts.[29] These materials combine the properties of M-NO units, such as reversible NO binding, with those of the porous hosts. Dispensing NO via photorelease mechanisms has been explored a lot recently, for instance, the photorelease of NO from nitrosothiol-derivatized surfaces,[30] Roussin's salts,[31] Fe–NO porphyrins,[32] Ru–NO complexes,[33] and Cr^{III}–nitrite complexes.[34] Frost and Meyerhoff[35] described the first hydrophobic NO-releasing material that used light as an external on/off trigger to control the flux of NO generated from cured polymer films. Borovik and coworkers[36] synthesized a new functional polymer P-1[Co^{II}(salen)] containing discrete recognition sites with coordinative unsaturated Co^{II} centers by molecular imprinting method. The reversible binding of the immobilized four-coordinate Co^{II} sites inside P-1[Co^{II}(salen)] to NO was confirmed by electronic absorbance spectra and electron paramagnetic resonance. They demonstrated the selective binding affinity of P-1[Co^{II}(salen)] to NO relative to the biologically important gases oxygen (O_2), carbon dioxide (CO_2), and carbon monoxide (CO) by gas uptake measurements. They also studied the release percent of the material for NO and found that at room temperature and atmospheric pressure, 40% conversion of P-1[Co(salen)NO] to P-1[CoII(salen)] was achieved in 14 days, but under vacuum at 120°C, this conversion was completed in about 1 h, whereas P-1(salen), without Co^{II} ions coordinated to the immobilized salen sites, only had nonselective physical adsorption for these gases. To make better use of the imprinted polymer as NO storage-release and sensing material, we further investigated the thermodynamic and kinetic characteristics of P-1[Co^{II}(salen)]'s binding to NO by means of GC/MS. The proposed kinetic and thermodynamic mechanisms were evaluated by Lagergren equation and Langmuir and Freundlich isotherm models.

EXPERIMENTAL

Chemicals

All solvents and chemicals used were of analytical grade, purchased from commercial sources and used directly unless otherwise noted. Methanol, trichloromethane, ethylenediamine, ether, 1,2-dichloroethane, and *N*,*N*-dimethylformamide (DMF) were dried according to previous standard procedures.[37] $Co(OAc)_2{\cdot}4H_2O$ was dehydrated by heating to 120°C under vacuum for 48 h. 2,4-Dihydroxybenzaldehyde was obtained from Aldrich (Milwaukee, Wisconsin) and purified by recrystallization. 4-Dimethylaminopyridine used in the synthesis was purified by recrystallization from toluene. Ethylene glycol dimethacrylate (EDMA) and methacrylic acid were purchased from Sigma-Aldrich (St. Louis, Missouri) and distilled in vacuum before use to remove inhibitors. 2,2′-Azobisisobutyronitrile (AIBN) was purchased from Tianjin Beilian Fine Chemicals and recrystallized from methanol. Ferrocenium hexafluorophosphate and 4-(chloromethyl)styrene were obtained from Sigma-Aldrich (St. Louis, Missouri). NO (99.99%) was obtained from Tianjin Summit Specialty Gases Co. Ltd. (Tianjin/China). Manipulations involving air-sensitive materials and syntheses of complexes and polymers were performed in a dry box in the flow of nitrogen gas.

Instruments

Nicolet 380 Fourier transform infrared (FTIR) spectroscopy (Thermo, Massachusetts), Tnova-600 nuclear magnetic resonance spectrometer (Varian, Palo Alto/California), DTG-60/60AH thermogravimetric analyzer (TGA; Shimadzu, Japan), Q10 differential scanning calorimeter (DSC; TA, New Castle/Delware), and 450GC-300MS gas chromatography mass spectra apparatus (Varian, Palo Alto/California) were used.

GC/MS Operation Conditions

The quantitative analysis of NO was done by GC/MS. Gas chromatographic (GC) separation was carried out with a capillary chromatographic column (30 m × 0.25 mm, and 0.25-μm film thickness of 5% diphenyl and 95% dimethyl polysiloxane; Varian, Palo Alto/California). Helium was used as carrier gas with a flow rate of 1.0 mL/min at a pulse pressure of 10.0 psi, and pulse duration was 0.25 min. In the GC system, the split/splitless injector (Varian 1177, Palo Alto/California) was operated in split mode with a split ratio of 1: 20. The injector and column temperatures were 50.0 and 25.0°C, respectively. Mass spectrometer was operated in electronic impact mode at 70 eV scanning the 20–50 m/z range. The temperature of MS quadrupole detector was 250.0°C.

Synthesis of Intermediates and P-1[Co^{II}(salen)]

According to the procedures reported previously,[22,36,38,39] the intermediates and the aim polymer P-1[Co^{II}(salen)][36] were synthesized (Scheme 1).

2-Hydroxy-4-(4-vinylbenzyloxy)benzaldehyde. The reaction was carried out in a 500-mL three-necked flask reactor equipped with a reflux condenser and nitrogen gas purge line. 2,4-Dihydroxybenzaldehyde (7.2 g, 0.0435 mol) was dissolved in

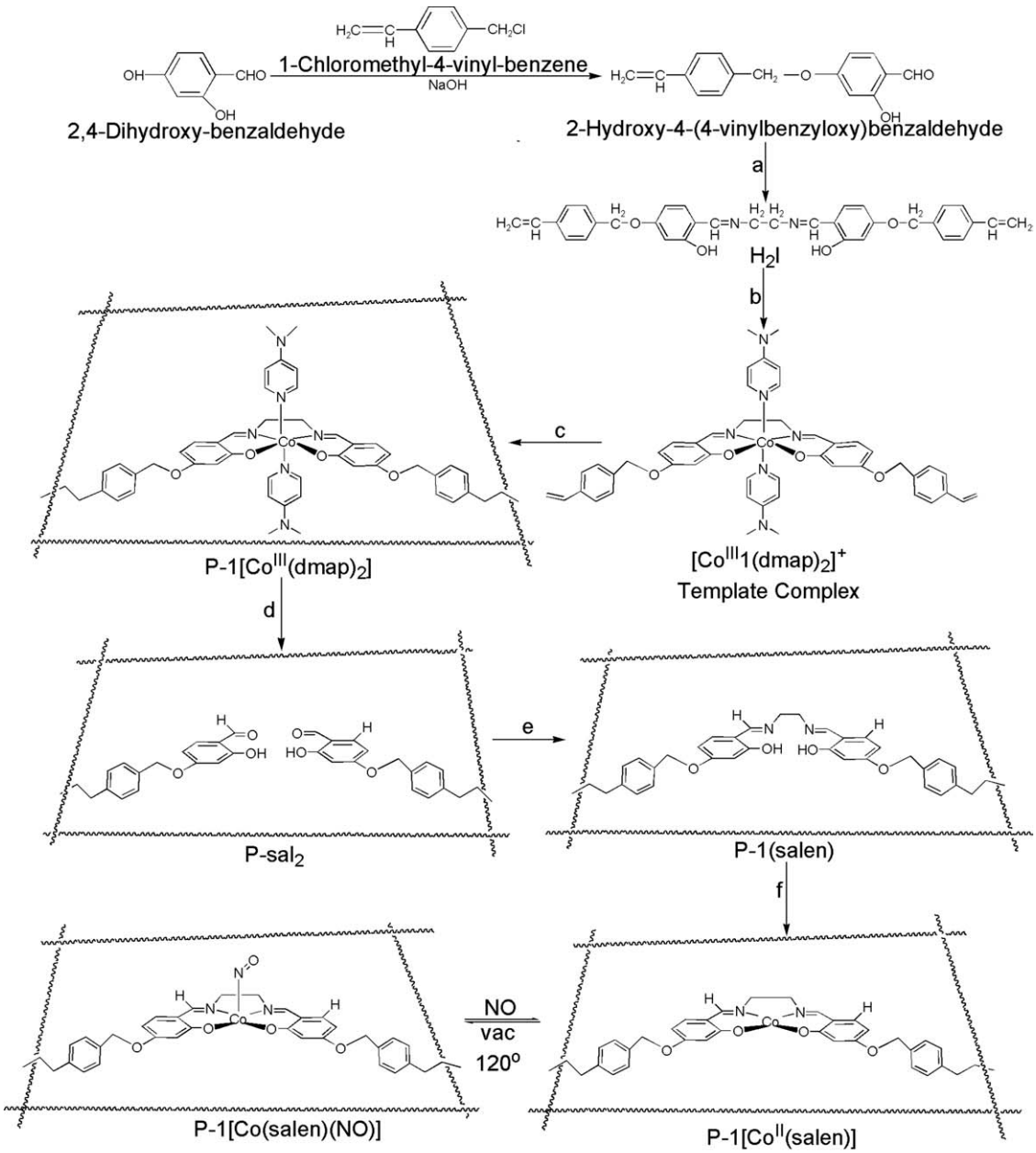

Scheme 1. Synthetic illustration of the intermediate compounds and P-1[Co^{II}(salen)].

300 mL of ethanol, and then, one equivalent of 4-vinylbenzyl chloride (8.0 g, 0.0522 mol) was added. After the mixture became transparent, 72 mL of 0.1*M* aqueous sodium hydroxide solution was added dropwise, and then, the solution was refluxed for 24 h, cooled, and filtered. After removal of ethanol from the filtrate under vacuum, 40 mL of petroleum ether was added into the residue, heated, and 1.82 g of 2-hydroxy-4-(4-vinylbenzyloxy)benzaldehyde was crystallized from the cooled solution with a yield of 13.73%. mp: 99°C. FTIR and ^{1}H-NMR spectra of the compound were measured to identify its chemical structure. FTIR (KBr), wavenumbers (cm^{-1}): 3414 (s), 2838 (m), 1643 (vs), 1664 (s), 1224 (s), 1019 (m). ^{1}H-NMR ($CDCl_3$): δ 5.1 (s, 2H), 5.27 (s, 1H), 6.39 (s, 1H), 6.48 (m, 2H), 6.60 (d, 1H), 6.70 (dd, 1H), 7.37 (d, 2H), 7.42 (d, 1H), 7.44 (d, 2H), 9.71 (s, 1H).

Bis[2-hydroxy-4-(4-vinylbenzyloxy)benzaldehyde]ethylenediimine ($H_2$1). 2-Hydroxy-4-(4-vinylbenzyloxy)benzaldehyde (1.80 g 7.073 mmol) and 27 mL of freshly dried methanol were added orderly to a 100-mL dry two-necked round-bottomed flask and stirred vigorously under nitrogen gas. Anhydrous ethylenediamine (3.6 mmol, 0.234 mL) was added to the suspension mixture via a

syringe and a bright yellow solution was produced, and then a yellow solid appeared immediately. After being stirred for 4 h, the reaction mixture was filtered through a medium porosity frit filter and a stratiform yellow precipitate was obtained. Trichloromethane was added till the solid was dissolved completely. Then diethyl ether was added into the trichloromethane solution dropwise and pure $H_2$1 was dissolved out. Filtration and dryness under vacuum yielded 1.223 g of $H_2$1 (86.93% yield). mp: 178°C. FTIR (KBr), wavenumbers (cm^{-1}): 3444 (vs), 1638 (s), 1613 (s), 1576 (w), 1514 (w), 1217(w), 1180 (m). ^{1}H-NMR ($CDCl_3$): δ 3.86 (s, 4H), 5.04 (s, 4H), 5.25 (d, 2H), 5.74 (d, 2H), 6.43 (dd, 2H), 6.50 (d, 2H), 6.69 (dd, 2H), 7.09 (d, 2H), 7.36 (m, 4H), 8.20 (s, 2H), 13.62 (s, 2H). The IR and ^{1}H-NMR spectra were in good agreement with the previously reported spectra.[22]

[Co1(dmap)$_2$][PF$_6$] (dmap: N,N′-dimethyl-4-aminopyridine). The following reaction was carried out in a dry 250-mL single-necked round-bottomed flask under nitrogen gas atmosphere. $H_2$1 (1.159 g, 2.232 mmol) was partially dissolved in 35 mL of anhydrous 1,2-dichloroethane, giving a yellow suspension. A purple solution of $Co(OAc)_2$ (0.395 g, 2.23 mmol) in 12.5 mL of methanol was added dropwise to the mixture while stirring, and the color of the mixture changed from yellow to red-orange and then to intensely dark brown after the addition was completed. Then, 12.5 mL of the methanolic solution containing 0.545 g (4.465 mmol) of 4-(dimethylamino)pyridine and 35 mL of the deep-blue methanolic suspension of 0.739 g (2.23 mol) ferrocenium hexafluorophosphate were added to the mixture sequentially without appreciable color change. The reaction mixture was stirred for additional 12 h at room temperature and then concentrated under reduced pressure, yielding a brown solid. After filtered, the solid was washed five times with diethyl ether, three times with a 3: 1 diethyl ether: methanol solution, and twice with diethyl ether orderly. The solid was dried under vacuum overnight to yield 1.91 g (1.95 mmol, 86.92% yield). FTIR (KBr), wavenumbers (cm^{-1}): 3081 (w), 2926 (w), 2868 (w), 1626 (s), 1604 (s), 1541 (m), 1484 (w), 1431 (m), 1388 (m), 1307 (w), 1262 (w), 1225 (s), 1185 (m), 1144 (w), 1124 (m), 1043 (m), 1021 (m), 952 (w), 915 (w), 843 (s) cm^{-1}. ^{1}H-NMR (DMSO): δ 8.17 (s, 2H), 7.52 (d, 4H), 7.43 (m, 8H), 7.20 (d, 2H), 6.75 (d, 2H), 6.68 (dd, 2H), 6.50 (d, 4H), 6.22 (dd, 2H), 5.87 (d, 2H), 5.29 (d, 2H), 5.08 (s, 4H), 3.97 (s, 4H), 2.91 (s, 12H), which were consistent with that reported previously.[36]

P-1[Co^{III}(dmap)$_2$]. The synthesis of P-1[Co^{III}(dmap)$_2$] was carried out by adding 1.58 g (1.618 mmol) of [Co1(dmap)$_2$][PF_6] (template complex) to a single-necked round-bottomed flask. Then, 18 mL of DMF (porogen) was added under nitrogen gas atmosphere, and the solution was stirred for 5 min. Finally, 6.422 g (32.4 mmol) of EDMA (crosslinker) and 0.056 g (0.343 mmol) of AIBN (initiator) were added. The mixture was then transferred to a thick-walled pressure Amp-bottle, and nitrogen gas was purged into the solution for 10 min. The Amp-bottle was sealed under vacuum and kept in a water bath at 60°C for 24 h, at which point a highly crosslinked polymer was formed in the tube. After removal of DMF under vacuum, the resulting bulk rigid polymer was crushed and ground manually with a mortar and pestle. The resultant polymer was subjected to continuous Soxhlet extraction with 150 mL of methanol for 12 h to remove the unreacted reagents and template molecules. After dried in a vacuum oven, 6.95 g of the red-brown polymer was obtained.

P-sal$_2$. The removal of Co^{III} ions and the dmap ligands was achieved by refluxing P-1[Co^{III}(dmap)$_2$] (5.626 g) in 240 mL aqueous solution of 0.1*M* Na_2EDTA at a pH of about 4 for 24 h under nitrogen gas. The polymer was filtered and washed five times with deionized water, three times with methanol, and three times with diethyl ether orderly. After drying under vacuum, 4.92 g of the light-tan polymer (P-sal$_2$) was obtained.

P-1(salen). P-sal$_2$ (4.057 g) was suspended in 36 mL of freshly distilled methanol with one equivalent of freshly distilled ethylenediamine (54.36 μL, 810 μmol) under stirring and constant nitrogen purging for 6 h at room temperature, which yielded a yellow-tan polymer P-1(salen). After being filtered, washed three times with diethyl ether, and dried under vacuum for 15 min, 3.624 g of P-1(salen) was obtained. The predisposition of the salicylaldehyde groups allowed for regeneration of the salen ligands within the porous host.

P-1[Co^{II}(salen)]. The polymer P-1(salen) (1.081 g) was added into 12 mL of 0.1*M* methanolic anhydrous $Co(OAc)_2$ solution under nitrogen gas atmosphere and stirred at room temperature for 6 h. After filtered, the polymer was extracted repeatedly in a Soxhlet extractor with methanol for 12 h. The resultant polymer was dried under vacuum, ground, and sieved to the particle size distribution of less than 75 μm for the following experiments.

Binding Kinetics and Thermodynamics of P-1[Co^{II}(salen)]

To determine the contact time required to reach equilibrium, the binding dynamic experiments were carried out at 25°C. The sample bottle was prepared by inserting a small bottle containing 0.1000 g of P-1[Co^{II}(salen)] into the bottom of a wide-mouth bottle coupled with a rubber stopper. The wide-mouth bottle was completely filled with nitrogen gas by successively applying a vacuum and refilling with nitrogen gas for three times. Five microliters of the gaseous sample was drawn from the wide-mouth bottle via a gas-tight syringe and injected into the capillary column of GC-MS in split mode immediately. NO (300 μL) was added via a gas-tight syringe into the wide-mouth bottle, and the concentration of NO was continuously monitored by GC/MS with respect to time. After the addition of NO, 5 μL of the gaseous sample was drawn from the wide-mouth bottle and analyzed by GC/MS every other 6 min. The peak area of *m*/*z* 30 of NO was measured for quantification of NO.

$$S_S = S_{S,NO} - S_{S,0}, \quad (1)$$

where $S_{S,NO}$ is the peak area after the addition of NO; $S_{S,0}$ is the peak area before the addition of NO; and S_S is the increment of peak area as a result of the addition of NO and adsorption by P-1[Co^{II}(salen)].

The preparation, measuring method, and data process of vacant wide-mouth bottles were the same as the sample bottles only without addition of P-1[Co^{II}(salen)]. Moreover, all the used wide-mouth bottles were with the equal volume.

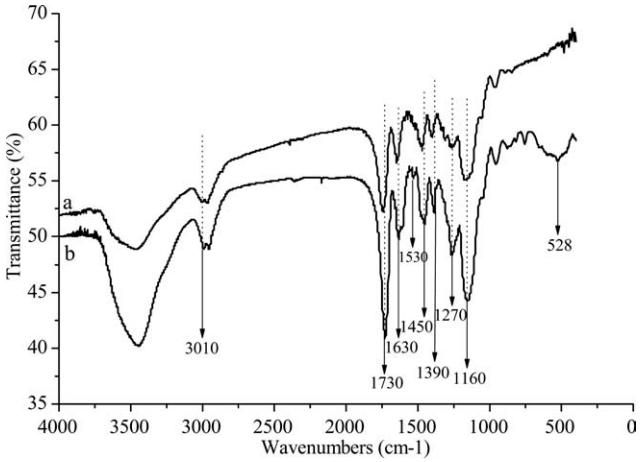

Figure 1. FTIR spectra of P-1(salen) (a) and P-1[Co^{II}(salen)] (b).

$$S_V = S_{V,NO} - S_{V,0}, \quad (2)$$

where $S_{V,NO}$ is the peak area after the addition of NO in the vacant bottle; $S_{V,0}$ is the peak area before the addition of NO; and S_V is the increment of the peak area resulting from the addition of NO.

Thus, the concentration of NO bound by P-1[Co^{II}(salen)], q (mol/g), each time can be calculated as follows:

$$q = \frac{V_0(S_V - S_S)}{mV_m S_V}, \quad (3)$$

where V_0 (L) is the added volume of NO; m (g) is the mass of P-1[Co^{II}(salen)]; and V_m (L/mol) is the molar volume of gas at room temperature.

In the binding equilibrium experiments, different volumes of NO, CO_2, or O_2 were added to the wide-mouth bottle, and previous procedures were repeated. The average data of triplicated independent results were used for further analysis.

Selectivity of P-1[Co^{II}(salen)]

O_2 and CO_2 were used to test and verify the selectivity of P-1[Co^{II}(salen)] because they are all biologically important gaseous compounds. The preparation, measuring method, and data process of samples and vacant bottles were the same as the procedures described above. About 300 μL of NO, O_2, or CO_2 was added into a wide-mouth bottle via a gas-tight syringe, and the amount of gases bound by P-1[Co^{II}(salen)] was determined by GC/MS according to the procedure of measurement of NO.

RESULTS AND DISCUSSION

Characterization of P-1[Co^{II}(salen)]

FTIR Analysis. The FTIR spectra of P-1(salen) (a) and P-1[Co^{II}(salen)] (b) were measured and are shown in Figure 1. The main functional groups of the predicted structure can be observed with corresponding infrared absorption peaks. The characteristic bands around 528 cm^{-1} of P-1[Co^{II}(salen)] are indicative to the presence of Co—N and Co—O bonds,[40] which suggest that Co(II) may be coordinated into P-1(salen). The peak around 1730 cm^{-1} is attributed to the stretching vibrations of —C=N—. The features around 3010, 1630, 1530, and 1450 cm^{-1} indicate the presence of benzene ring. The peaks at 1390, 1270, and 1160 cm^{-1} are attributed to the stretching vibrations of the —C—N—, Ar—O—, and —CH_2—O— bonds. When compared with the P-1(salen), the FTIR features of P-1[Co^{II}(salen)] show very similar position and appearance of the major bands.

Thermal Analysis. The thermal properties of P-1[Co^{II}(salen)] were studied by TGA and DSC. The TGA curve (temperature: 30–600°C; heating rate: 20°C/min) of dry P-1[Co^{II}(salen)] is given in Figure 2(A), from which we can see that P-1[Co^{II}(salen)] is thermally stable up to 300°C. Linear decrease in weight appears from ~300 to ~440°C because of the thermal decomposition of the polymer. Moreover, based on the weight loss obtained from the TGA analysis, the polymer frame content is estimated as high as 80.11 wt %. The P-1[Co^{II}(salen)] was placed in an incubator (23°C, 50% moisture) for 24 h to adjust the state of sample before the measurement of DSC at a heating rate of 10°C/min from 30 to 165°C under continuous flow of dry nitrogen gas. The DSC thermogram of P-1[Co^{II}(salen)] shown in Figure 2(B) indicates that the glass transition

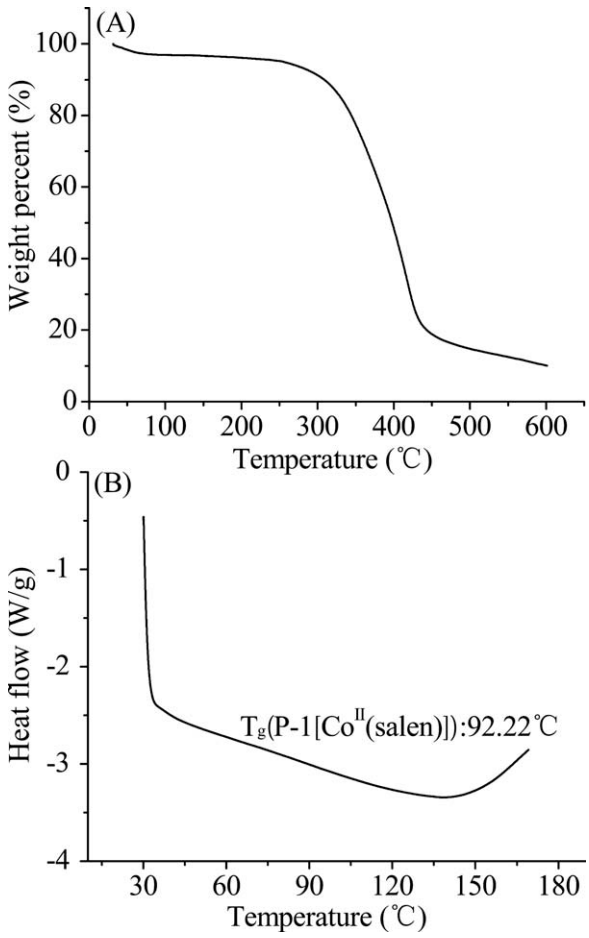

Figure 2. TGA curve (A) and DSC heating thermogram (B) of P-1[Co^{II}(salen)].

Applied Polymer SCIENCE

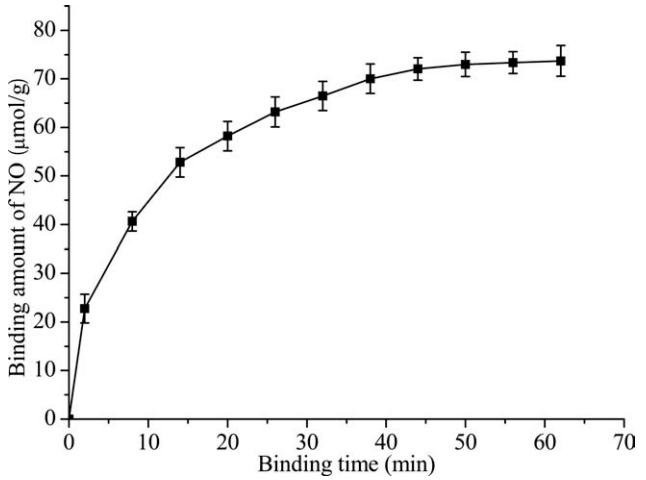

Figure 3. Dependence of the binding amount of 0.1000 g of P-1[Co^{II}(salen)] to NO on binding time at 25°C under N_2 atmosphere.

temperature (T_g) is 92.22°C. All these results demonstrate that the polymeric chain of P-1[Co^{II}(salen)] can move easily and P-1[Co^{II}(salen)] can tolerate high temperature.

Analyses for Binding Kinetics of P-1[Co^{II}(salen)] by First- and Second-Order Models

We monitored the binding amount of P-1[Co^{II}(salen)] to NO with respect to time (Figure 3). Figure 3 shows that the binding occurs rapidly in the first 20 min, after which the binding rate starts to slow down; almost 60% of the total amount of NO is bound at 44 min when the binding of P-1[Co^{II}(salen)] to NO reaches an equilibrium. Therefore, the binding time was selected as 44 min for the following equilibrium experiments. To evaluate the kinetic binding mechanism, the first-order and second-order models[41,42] of the Lagergren method are used:

$$\ln\frac{q_e}{q_e - q_t} = k_1 t, \tag{4}$$

$$\frac{q_t}{q_e(q_e - q_t)} = k_2 t, \tag{5}$$

where q_t and q_e (μmol/g) are the amounts of bound NO at time t and at equilibrium, respectively, which can be calculated by subtracting the free NO from the initial NO concentration; and k_1 and k_2 are the binding rate constants for the first- and second-order models, respectively. The rate constants (k_1 and k_2) of the binding reaction between NO and P-1[Co^{II}(salen)] and the correlation coefficients calculated using linearized plots of eqs. (4) and (5) are shown in Table I.

Table I. Comparison of First- and Second-Order Kinetic Models for Binding of P-1[Co^{II}(salen)] to NO

Kinetic models	k_1 (min^{-1}) or k_2 [g/(mmol min)]	r^2	χ^2
First order	0.09 ± 0.01	0.98 ± 0.34	0.01 ± 0.01
Second order	23.76 ± 5.90	0.76 ± 629.70	0.02 ± 0.01

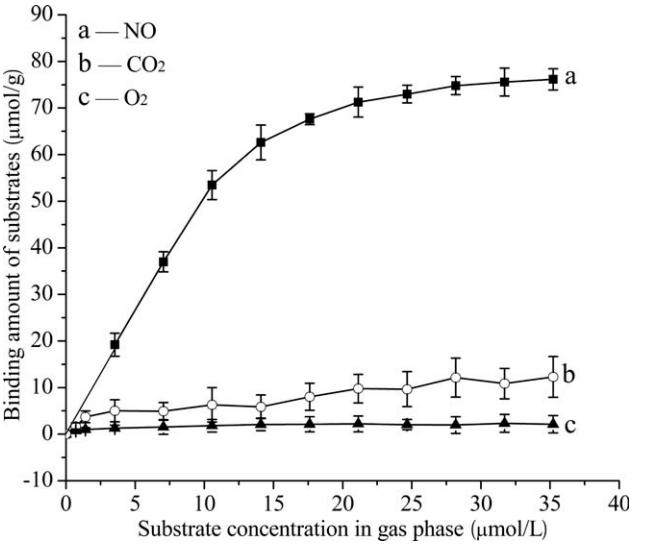

Figure 4. Effect of NO, CO_2, and O_2 concentrations in gas phase on the binding capacity of P-1[Co^{II}(salen)] at 25°C under N_2 atmosphere, taking 44 min as binding time.

According to the correlation coefficients, the first-order model (r^2 = 0.980) fits the experimental data much better than the second-order model (r^2 = 0.758). To select the most appropriate kinetic model, χ^2 test was also done by eq. (6)[21,43]

$$\chi^2 = \sum\frac{(q_t - q_{tm})^2}{q_{tm}}, \tag{6}$$

where q_t and q_{tm} (μmol/g) are total NO binding capacities at time t obtained from the experimental data and the kinetic model, respectively. It can be seen from Table I that the errors between calculated and experimental values (χ^2) are less for the first-order model, which suggests that the first-order kinetic model better fits the binding of P-1[Co^{II}(salen)] to NO. Together with the comparison of correlation coefficients (r^2) listed above, this suggests that the binding system is not a second-order reaction and is the first-order model.

Analyses for Binding Thermodynamics by Langmuir and Freundlich Isotherm Models

To investigate the effect of NO concentration in gas phase on binding capacity of P-1[Co^{II}(salen)], the binding amount of P-1[Co^{II}(salen)] particles to NO was determined with increasing initial NO concentration (Figure 4). As shown in Figure 4, the maximum binding capacity of the P-1[Co^{II}(salen)] to NO was measured to be about 75 μmol/g of polymers.

There are several isotherm models used for description of the thermodynamic binding mechanism for a sorbent.[44] Langmuir and Freundlich models[44] were used in the current study. These two isotherm equations can be expressed as follows:

$$\text{Langmuir model}: B = \frac{K_L B_{\max}[\text{NO}]}{1 + K_L[\text{NO}]}. \tag{7}$$

Equation (7) can be rewritten as follows:

Table II. Isotherm Constants for Substrates Adsorption by P-1[Co^{II}(salen)]

Substrates	Langmuir constants				Freundlich constants			
	B_{max} (μmol/g)	K_L (L/μmol)	r^2	χ^2	n	K_F	r^2	χ^2
NO	76.28 ± 1.30	1.57 ± 0.03	1.00 ± 0.01	0.36 ± 0.01	3.79 ± 0.52	38.58 ± 2.86	0.94 ± 0.17	10.07 ± 1.67
CO_2	12.47 ± 0.50	0.39 ± 0.02	0.95 ± 0.05	0.52 ± 0.12	1.82 ± 0.12	3.22 ± 0.77	0.90 ± 0.36	0.41 ± 0.36
O_2	1.51 ± 0.17	0.61 ± 0.07	0.99 ± 0.04	0.56 ± 0.09	3.06 ± 0.11	0.90 ± 0.16	0.99 ± 0.02	0.01 ± 0.01

$$\frac{1}{B} = \frac{1}{K_L B_{max}[NO]} + \frac{1}{B_{max}}. \quad (8)$$

$$\text{Freundlich model}: B = K_F[NO]^{1/n}. \quad (9)$$

From eq. (9), we can obtain the following equation:

$$\ln B = \ln K_F + \frac{1}{n}\ln[NO], \quad (10)$$

where B (μmol/g) is the binding amount of NO at equilibrium; B_{max} (μmol/g) is an apparent maximum number of binding sites; [NO] (μmol/L) is the concentration of free NO at equilibrium; K_L is the Langmuir constant (L/μmol); K_F is the Freundlich constant; and $1/n$ is the Freundlich's intensity factor.[43,45] The value of n in the range of 1–10 denotes favorable adsorption. The experimental data were treated with eqs. (9) and (10), respectively; the Langmuir and Freundlich constants along with the correlation coefficients (r^2) were calculated. The results are presented in Table II. To select the most suitable isotherm model, χ^2 test was done by the following equation[21,43]:

$$\chi^2 = \sum \frac{(B - B_m)^2}{B_m}, \quad (11)$$

where B and B_m (μmol/g) are NO binding capacity at equilibrium from the experimental data and the isotherm models, respectively. The r^2 and χ^2 values in Table II suggest that total NO bound by P-1[Co^{II}(salen)] can be better fitted by the Langmuir equation. It implies that the polymer P-1[Co^{II}(salen)] has homogeneous binding sites for NO in the gas phase. The nonspecific binding sites can be assumed to be small enough to be ignored in the applied NO concentration range. The maximum binding capacity (B_{max}) of P-1[Co^{II}(salen)] is found to be about 76.28 μmol/g, which is very similar to the experimentally saturated value (75 μmol/g). In addition, to better understand the high affinity of the polymer on NO, the binding isotherms of P-1[Co^{II}(salen)] to CO_2 and O_2 are also shown in Figure 4. According to the Langmuir and Freundlich models, the obtained isotherm constants are given in Table II. Table II indicates that the Langmuir and Freundlich constants and the maximum binding capacities of CO_2 and O_2 are much too less than those of NO. This further demonstrates that P-1[Co^{II}(salen)] has very weak adsorption to CO_2 and O_2.

Selectivity of P-1[Co^{II}(salen)]

The binding selectivity of P-1[Co^{II}(salen)] to biologically important gaseous compounds, O_2, CO_2, and NO, was evaluated by the selectivity factor (α), which is defined as the ratio of the distribution coefficient of NO to those of other tested gases or itself. The distribution coefficients were calculated from the ratio of the concentration bound by P-1[Co^{II}(salen)] to that in gas phase for the same tested gas:

$$D = \frac{B}{[G]}, \quad (12)$$

$$\alpha = \frac{D_{NO}}{D_G}, \quad (13)$$

Table III. Selectivity Factors of P-1[Co^{II}(salen)] for Tested Gas (n = 3)

Substrates	NO	O_2	CO_2
D (L/g)	8.05 ± 0.29	0.11 ± 0.01	0.50 ± 0.02
α	1.00	75.97 ± 4.19	16.05 ± 2.14

where D_{NO} and D_G represent the distribution coefficient of NO and the tested gaseous compounds, respectively; B and [G] represent the bound and free amount of each gas. The higher the value of α, the better is the selectivity for NO. The D and α values of P-1[Co^{II}(salen)] for the tested gaseous molecules are summarized in Table III. These results indicate that P-1[Co^{II}(salen)] has very weak affinity to O_2 and CO_2. The strong interaction between P-1[Co^{II}(salen)] and NO may be due to the fact that the electron in the d_{z^2} orbital of the Co^{II} in P-1[Co^{II}(salen)] covalently bonds to the electron in the π^* orbital (a higher energy state) of NO.[46] In this process, the electrons of NO rearrange, and the intermolecular interaction is enhanced as a result of the increase in the polarity of NO molecule. As is well known, O_2 and CO_2 are apolar molecules whose molecular structures are obviously different from that of NO. Therefore, O_2 and CO_2 cannot covalently bind to the Co^{II} sites in square-planar arrangement. The results agree with the binding characters of the Co(II) salen-type metal complexes reported previously.[47–50] Therefore, the adsorption of P-1[Co^{II}(salen)] to O_2 or CO_2 is nonselective physical adsorption; however, the adsorption to O_2 and CO_2 were seldom observed in the experiments as P-1[Co^{II}(salen)] was saturated with nitrogen gas by physical adsorption in advance.

CONCLUSIONS

In conclusion, the polymer P-1[Co^{II}(salen)] was synthesized according to the procedures published previously. Its binding characteristics were investigated by the Lagergren method and the Langmuir and Freundlich models and compared with NO, CO_2, and O_2. The binding of P-1[Co^{II}(salen)] to NO corresponds with the Lagergren first-order kinetics. The polymer P-1[Co^{II}(salen)] has homogeneous binding sites for NO in gas phase. B_{max} of the polymer is found to be 76.28 μmol/g. The affinity of P-1[Co^{II}(salen)] to NO is very high when compared with CO_2 and O_2. It is expected that P-1[Co^{II}(salen)] is a promising functional material for NO storage and has a huge potential as a fast and sensitive NO-sensing element.

ACKNOWLEDGMENTS

This work was supported by a grant from the National Natural Science Foundation of China (No: 21175083).

REFERENCES

1. Shea, K. J. *Trends Polym. Sci. (Cambridge, UK)* **1994,** *2*, 166.
2. Mosbach, K. *Trends Biochem. Sci.* **1994,** *19*, 9.
3. Wulff, G.; Sarhan, A. *Angew. Chem. Int. Ed. Engl.* **1972,** *11*, 341.
4. Vlatakis, G.; Anderson, L. I.; Müller, R.; Mosbach, K. *Nature* **1993,** *361*, 645.
5. Praveen, R. S.; Daniel, S.; Rao, T. P. *Talanta* **2005,** *66*, 513.
6. Tamayo, F. G.; Titirici, M. M.; Martin-Esteban, A.; Sellergren, B. *Anal. Chim. Acta* **2005,** *542*, 38.
7. Djozan, D.; Ebrahimi, B.; Mahkam, M.; Farajzadeh, M. A. *Anal. Chim. Acta* **2010,** *674*, 40.
8. Xu, Z. X.; Fang, G. Z.; Wang, S. *Food Chem.* **2010,** *119*, 845.
9. Hart, B. R.; Rush, D. J.; Shea, K. J. *J. Am. Chem. Soc.* **2000,** *122*, 460.
10. Bhim, B. P.; Rashmi, M.; Mahavir, P. T.; Piyush, S. S. *Sens. Actuators B* **2010,** *146*, 321.
11. Wei, S.; Jakusch, M.; Mizaikoff, B. *Anal. Chim. Acta* **2006,** *578*, 50.
12. Ji, H. B.; Huang, Y. Y.; Qian, Y.; Wang, T. T.; Zhang, M. Y. *Chin. J. Chem. Eng.* **2006,** *14*, 118.
13. Liu, Y. W.; Chang, X. J.; Wang, S.; Guo, Y.; Din, B. J.; Meng, S. M. *Anal. Chim. Acta* **2004,** *519*, 173.
14. Wu, L. Q.; Li, Y. Z. *Anal. Chim. Acta* **2003,** *482*, 175.
15. Hoai, T. N.; Yoo, D. K.; Kim, D. *J. Hazard. Mater.* **2010,** *173*, 462.
16. Otero-Romaní, J.; Moreda-Piñeiro, A.; Bermejo-Barrera, P.; Martin-Esteban, A. *Microchem. J.* **2009,** *93*, 225.
17. Tada, M.; Iwasawa, Y. *J. Mol. Catal. A* **2003,** *199*, 115.
18. Jenkins, A. L.; Uy, O. M.; Murray, G. M. *Anal. Chem.* **1999,** *71*, 373.
19. Buhani; Narsito; Nuryono; Kunarti, E. S. *Desalination* **2010,** *251*, 83.
20. Otero-Romaní, J.; Moreda-Piñeiro, A.; Bermejo-Barrera, P.; Martin-Esteban, A. *Talanta* **2009,** *79*, 723.
21. Buhani; Suharso; Sumadi. *Desalination* **2010,** *259*, 140.
22. Sharma, A. C.; Borovik, A. S. *J. Am. Chem. Soc.* **2000,** *122*, 8946.
23. Armor, J. N. *Catal. Today* **1995,** *26*, 99.
24. Lincoln, J.; Hoyle, C. H. V.; Burnstock, G. Nitric Oxide in Health and Disease; Cambridge University Press: New York, **1997.**
25. Ignarro, L. J. Nitric Oxide: Biology and Pathobiology; Academic Press: New York, **2000.**
26. Wink, D. A.; Mitchell, J. B. *Free Radical Biol. Med.* **1998,** *25*, 434.
27. Ding, X. D.; Weichsel, A.; Andersen, J. F.; Shokhireva, T. K.; Balfour, C.; Pierik, A. J.; Averill, B. A.; Montfort, W. R.; Walker, F. A. *J. Am. Chem. Soc.* **1999,** *121*, 128.
28. Zhang, H.; Annich, G. M.; Miskulin, J.; Stankiewicz, K.; Osterholzer, K.; Merz, S. I.; Bartlett, R. H.; Meyerhoff, M. E. *J. Am. Chem. Soc.* **2003,** *125*, 5015.
29. Wulff, G. *Angew. Chem. Int. Ed. Engl.* **1995,** *34*, 1812.
30. Etchenique, R.; Furman, M.; Olabe, J. A. *J. Am. Chem. Soc.* **2000,** *122*, 3967.
31. Bourassa, J.; DeGraff, W.; Kudo, S.; Wink, D. A.; Mitchell, J. B.; Ford, P. C. *J. Am. Chem. Soc.* **1997,** *119*, 2853.
32. Hoshino, M.; Ozawa, K.; Seki, H.; Ford, P. C. *J. Am. Chem. Soc.* **1993,** *115*, 9568.
33. Welbes, L. L.; Borovik, A. S. *Acc. Chem. Res.* **2005,** *38*, 765.
34. Leo, M. D.; Ford, P. C. *J. Am. Chem. Soc.* **1999,** *121*, 1980.

35. Frost, M. C.; Meyerhoff, M. E. *J. Am. Chem. Soc.* **2004,** *126*, 1348.
36. Padden, K. M.; Krebs, J. F.; MacBeth, C. E.; Scarrow, R. C.; Borovik, A. S. *J. Am. Chem. Soc.* **2001,** *123*, 1072.
37. Perrin, D. D.; Armarego, W. L. F. Purification of Laboratory Chemicals, 3rd ed.; Pergamon Press: New York, **1988.**
38. Daly, J.; Horner, L.; Witkop, B. *J. Am. Chem. Soc.* **1961,** *83*, 4787.
39. Krebs, J. K. PhD Thesis, Kansas State University, Manhattan, KS, **1998.**
40. Zhang, Y. L.; Ruan, W. J.; Zhao, X. J.; Wang, H. G.; Zhu, Z. A. *Polyhedron* **2003,** *22*, 1535.
41. Chiou, M. S.; Li, H. Y. *Chemosphere* **2003,** *50*, 1095.
42. Li, Q.; Liu, H. N.; Liu, T. Y.; Guo, M.; Qing, B. J.; Ye, X. S.; Wu, Z. J. *J. Chem. Eng.* **2010,** *157*, 401.
43. Kumar, P. A.; Ray, M.; Chakraborty, S. *J. Hazard. Mater.* **2007,** *143*, 24.
44. Mall, I. D.; Srivastava, V. C.; Agarwal, N. K. *Dyes Pigments* **2006,** *69*, 210.
45. Aklil, A.; Mouflih, M.; Sebti, S. *J. Hazard. Mater.* **2004,** *112*, 183.
46. Hoshino, M.; Konishi, R.; Tezuka, N.; Ueno, I.; Seki, H. *J. Phys. Chem.* **1996,** *100*, 13569.
47. Carter, M. J.; Rillema, P. P.; Basolo, F. *J. Am. Chem. Soc.* **1974,** *96*, 392.
48. Meier, I. K.; Pearlstein, R. M.; Ramprasad, D.; Pez, G. P. *Inorg. Chem.* **1997,** *36*, 1707.
49. Cesarotti, E.; Gullotti, M.; Pasini, A.; Ugo, R. *J. Chem. Soc. Dalton Trans.* **1977, 757.**
50. Musie, G. T.; Wei, M.; Subramaniam, B.; Busch, D. H. *Inorg. Chem.* **2001,** *40*, 3336.